Phase contrast soft x-ray microscopy using Zernike zone plates

Anne Sakdinawat^{1,2,*} and Yanwei Liu²

¹University of California San Francisco and University of California Berkeley Joint Graduate Group in Bioengineering, Berkeley, California 94720, USA

²NSF ERC for Extreme Ultraviolet Science and Technology, University of California Berkeley, and Center for X-ray Optics, Lawrence Berkeley National Laboratory, Berkeley, California 94720, USA

*Corresponding author: aesakdinawat@lbl.gov

Abstract: Soft x-ray Zernike phase contrast microscopy was implemented using a "Zernike zone plate" (ZZP) without the use of a separate phase filter in the back focal plane. The ZZP is a single optic that integrates the appropriate $\pm \pi/2$ radians phase shift through selective zone placement shifts in a Fresnel zone plate. Imaging using a regular zone plate, positive ZZP, and negative ZZP was performed at a wavelength of $\lambda = 2.163$ nm. Contrast enhancement with the positive ZZP and contrast reversal with the negative ZZP were observed.

©2008 Optical Society of America

OCIS codes: (340.7460) X-ray microscopy; (340.0340) X-ray optics; (050.1965) Diffractive lenses

References and links

- D. Attwood, Soft x-rays and extreme ultraviolet radiation: principles and applications, (Cambridge University Press, 1999).
- P.A.C. Jansson, U. Vogt, and H.M. Hertz, "Liquid nitrogen jet laser plasma source for compact soft x-ray microscopy," Rev. Sci. Instrum. 76, 043503 (2005).
- Energetiq Technology, Inc., "EQ-10M Soft X-ray & EUV Source," http://www.energetiq.com/DataSheets/DS004_EQ-10M_Data_Sheet_SXR.pdf.
- G. Schmahl, D. Rudolph, P. Guttmann, G. Schneider, J. Thieme, and B. Niemann, "Phase contrast studies of biological specimens with the x-ray microscope at BESSY," Rev. Sci. Instrum. 66, 1282-1286 (1995).
- G. Schmahl, D. Rudolph, G. Schneider, P. Guttmann, and B. Niemann, "Phase contrast X-ray microscopy studies," Optik 97, 181-182 (1994).
- M. Awaji, Y. Suzuki, A. Takeuchi, H. Takano, N. Kamijo, S. Tamura, and M. Yasumoto, "Zernike-type X-ray imaging microscopy at 25 keV with Fresnel zone plate optics," J. Synchrotron Rad. 9, 125-127 (2002).
- H. Yokosuka, N. Watanabe, T. Ohigashi, Y. Yoshida, S. Maeda, S. Aoki, Y. Suzuki, A. Takeuchi and H. Takano, "Zernike-type phase-contrast hard X-ray microscope with a zone plate at the Photon Factory," J. Synchrotron Rad. 9, 179-181 (2002).
- U. Neuhäusler, G. Schneider, W. Ludwig, M.A. Meyer, E. Zschech, and D. Hambach, "X-ray microscopy in Zernike phase contrast mode at 4 keV photon energy with 60 nm resolution," J. Phys. D: Appl. Phys. 36, A79-A82 (2003).
- Y. Kohmura, A. Takeuchi, H. Takano, Y. Suzuki, and T. Ishikawa, "Zernike phase-contrast X-ray microscope with an X-ray reflractive lens," J. Phys. IV France 104, 603-606 (2003).
- H.S. Youn and S-W. Jung, "Hard X-ray microscopy with Zernike phase contrast," J. Microsc. 223, 53-56 (2006).
- E. Di Fabrizio, D. Cojoc, S. Cabrini, B. Kaulich, J. Susini, P. Facci, T. Wilhein, "Diffractive optical elements for differential interference contrast x-ray microscopy," Opt. Express 11, 2278-2288 (2003).
- U. Vogt, M. Lindblom, P.A.C. Jansson, T.T. Tuohimaa, A. Holmberg, H.M. Hertz, M. Wieland, and T. Wilhein, "Single-optical-element soft x-ray interferometry with a laser-plasma x-ray source," Opt. Lett. 30, 2167-2169, (2005).
- C. Chang, A. Sakdinawat, P. Fischer, E. Anderson, and D. Attwood, "Single-element objective lens for soft x-ray differential interference contrast microscopy," Opt. Lett. 31, 1564-1566 (2006).
- A. Sakdinawat and Y. Liu, "Soft x-ray microscopy using spiral zone plates," Opt. Lett. 32, 2635-2637 (2007).

1. Introduction

Soft x-ray and hard x-ray microscopy enable high resolution imaging of samples with elemental specificity, time resolution, and spectroscopic capabilities [1]. Phase contrast imaging methods, as in visible light microscopy, are important for contrast enhancement in both the soft x-ray and hard x-ray regions. In the soft x-ray regime, most samples are complex, exhibiting both amplitude and phase properties. Contrast enhancement in this region allows for reduced exposure time, important in the case of imaging using compact sources [2,3] that may have lower brightness than a synchrotron source and for reduced radiation dose when studying radiation-sensitive samples [4]. In the hard x-ray regime, samples generally become more transparent and are primarily phase objects. Phase contrast, then, becomes the primary contrast-generating mechanism in image formation. A variety of phase sensitive techniques have been implemented for lens-based full-field x-ray microscopes including both Zernike phase contrast [5-10] and differential phase contrast imaging methods [11-14]. Use of single-element diffractive optical elements [11-14] to generate phase contrast is an attractive method of implementing phase-sensitive imaging due to the simplicity and ease in alignment. In this paper, Zernike phase contrast [15] imaging is performed using a single element objective, the Zernike zone plate, without the use of a separate phase filter.

2. X-ray Zernike phase contrast microscopy

Both soft x-ray and hard x-ray Zernike phase contrast microscopes have traditionally been implemented using hollow cone illumination and an imaging objective in combination with a separate $\pm \pi/2$ phase ring [5-10]. The phase ring has dimensions that match the geometry of the undiffracted light (0th order) from the sample and is generally placed at the back focal plane of the imaging objective. However, in many x-ray microscopes, the illumination is well collimated, resulting in good spatial constraint of the 0th order. This spatial constraint allows filtering to occur in planes other than the back focal plane of the objective, resulting in a larger tolerance for the longitudinal placement of the phase ring as compared to Köhler illumination in a typical visible light Zernike phase contrast implementation. It also allows the possibility of combining the phase plate and imaging objective into a single optical element.

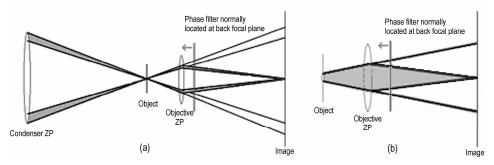


Fig. 1. (a) Schematic of a typical x-ray microscope with well-collimated hollow cone illumination. The 0th order contribution to the image is the light shaded in gray after the objective zone plate. This is the light that is filtered (typically with a phase ring) to provide the phase contrast. Other 0th order light from the sample that is not focused by the objective zone plate passes straight through, but does not contribute to the image since the image area at the CCD does not overlap that of the 0th order. The lack of large spatial divergence of the 0th order allows the phase filter to be moved from the back focal plane to the plane of the objective zone plate as shown by the arrow. This allows the combination of the phase filter and objective into a single optical element. (b) Schematic for the case of a microscope with on-axis illumination.

3. Zernike zone plate

In the soft x-ray regime, where materials generally exhibit a large absorption for a given amount of phase shift, the design of phase rings involves tradeoffs between a sufficient phase shift and the associated amount of beam attenuation. One way of overcoming this tradeoff is to incorporate the $\pm \pi/2$ phase shift directly into the zone plate imaging objective, making the "Zernike zone plate" (ZZP). The phase shift is incorporated by shifting the zone placement in a region of the zone plate rather than by material transmission from a separate filter. The shifted portion of the zone plate corresponds to the region of 0th order light determined by the illuminating geometry of the system. For example, an annular illumination intersecting the objective zone plate with an outer radius of r_{out} and an inner radius of r_{in} will have a shifted region approximately corresponding to an annulus with those dimensions. Both positive and negative Zernike-type phase contrast can be implemented by phase shifting the zones either by $+ \pi/2$ or $- \pi/2$, respectively.

Mathematically, the ZZP can be described by the following equations:

$$ZZP(r) = RZP(r)H_{ZZP}(r_{in}, r_{out})$$
(1)

where RZP(r), the regular zone plate, is given by:

$$RZP(r) = \exp\left(\frac{i\pi r^2}{\lambda f}\right) \tag{2}$$

and H_{ZZP}(r), the Zernike phase filter, is given by:

$$H_{ZZP}(r_{in}, r_{out}) = \begin{cases} \exp\left(\pm \frac{i\pi}{2}\right) & \text{if } r \leq r_{out} \text{ and } r \geq r_{in} \\ 1 & \text{for all other } r \end{cases}$$
 (3)

where λ is the wavelength of the radiation, f is the focal length of the lens, r_{out} is the outer radius of the phase filter, and r_{in} is the inner radius of the phase filter. The zone plates are then binarized due to fabrication constraints.

In the case of on-axis illumination, $r_{in} = 0$ and r_{out} corresponds to the 0th order of the sample, which is a small portion in the center area of the zone plate. This is illustrated in Fig. 2.

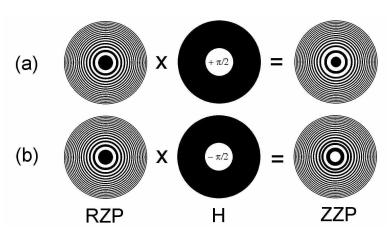


Fig. 2. Modification of a regular zone plate to a Zernike zone plate involves multiplying by a phase filter with shape and area corresponding to the undiffracted illumination used in the imaging system. The case of on-axis illumination is depicted for the positive Zernike phase contrast case (a) and for the negative Zernike phase contrast case (b). It can be seen that only the portion of the zone plate modified by the phase filter (in this case, the central area) is changed.

4. Zernike phase contrast experimental setup

The experiments reported here demonstrate both positive and negative Zernike-type phase contrast imaging using ZZPs. Three zone plates were designed and fabricated: a regular zone plate (RZP), a positive Zernike zone plate (PZZP), and a negative Zernike zone plate (NZZP). The zone plates were used to image a chromium test sample in a full-field soft x-ray microscope, and the resulting images were compared.

A schematic of the microscope is shown in Fig. 3 and is located at beamline 12.0.2.1 at the Advanced Light Source in Berkeley. The beamline source is an 8 cm undulator that generates soft x-rays from 200 eV to 1 keV. A varied line space plane grating monochromater was then used to tune the radiation to 2.163 nm with a spectral bandwidth of $\Delta\lambda/\lambda\approx 1/400$. The beam was focused into the experimental chamber to a final spot size of 80 x 10 um using a pair of Kirkpatrick-Baez mirrors. The chromium (Cr) grating sample and the zone plates were placed in an appropriate imaging geometry to provide 525 times magnification, and a CCD was used to record the images.

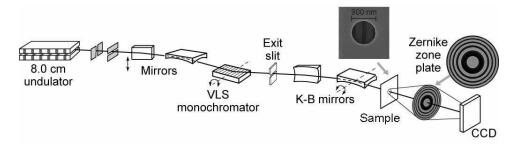


Fig. 3. Schematic of the experimental setup for the soft x-ray Zernike phase contrast microscope. A SEM image of a 45 nm thick Cr grating sample underneath a 900 nm Au pinhole is shown. The regular zone plate and Zernike zone plates were used to image the sample with a magnification of 525 times.

5. Zone plate and sample fabrication

The three aforementioned zone plate lenses were fabricated using the Nanowriter, an electron beam lithography system at the Center for X-ray Optics, Lawrence Berkeley National Laboratory. Each zone plate was designed to have 300 zones, an outermost zone width of 72 nm, and a diameter of 86.7 um. The focal length at $\lambda = 2.163$ nm is 2.876 mm. The phase-shifted zones are designed for on-axis illumination, with $r_{in} = 0$. We use $r_{out} = 4 \mu m$, which is to intersect the 0th order light from a Cr grating sample illuminated by a 900 nm pinhole.

The substrate for each of the zone plates was a 100 nm thick silicon nitride membrane with a plating base consisting of 5 nm chromium and 12 nm gold. Hydrogen silsesquioxane (HSQ), a negative electron beam resist, was used for patterning, and the electron beam exposure was performed. The resist was then developed using a solution of tetramethyl ammonium hydroxide (TMAH), and the zone plates were electroplated with 250 nm thick nickel. The remaining resist was stripped in a buffered hydrofluoric acid (BHF) solution. Scanning electron microscope (SEM) images of the zone plates are shown in Fig. 4.

The Cr test sample was also fabricated using electron beam lithography and consisted of approximately 45 nm thick Cr lines placed behind a 900 nm diameter gold pinhole aperture. A 100 nm thick silicon nitride membrane was used as the substrate for the sample. HSQ was used as the resist, a grating pattern was exposed using the Nanowriter, and the resist was developed using a TMAH solution. 45 nm Cr was then electron beam evaporated on the membrane and resist structure, and liftoff was performed in a BHF solution. A 900 nm diameter gold pinhole was then formed on top of the Cr test pattern through an overlaid exposure. A layer of a chemically amplified negative e-beam resist AZPN114 was spun onto the wafer with the Cr patterns, alignment in the Nanowriter was performed to ensure overlap

between the first pattern and the pinhole, and the pinholes were exposed. After the exposure, a post exposure bake of 5 min at 105C was performed, and the resist was developed in a solution of MF312. 10 nm Au was the evaporated onto the wafer and resist structure to form a suitable plating base. Then, 1 μ m thick Au was electroplated to form the pinholes. Finally, the resist was stripped using an acid piranha solution. A SEM image of the test pattern is shown in Fig. 3.

6. Experimental results

Images of the test sample were taken with each of the three zone plates: the RZP, PZZP, and NZZP at a wavelength of $\lambda=2.163$ nm. Resulting images from the experiment, along with corresponding SEM images of the zone plates, are shown in Fig. 4. Line profiles in the three cases were compared. Modulation of the regular zone plate image was 34% and modulation for the PZZP was 53%. In the case of the NZZP, contrast reversal was seen and the modulation was 22%. Line profiles are seen in Fig. 5.

At 2.163 nm, the Cr line has a fairly large phase contribution. With a thickness of 45 nm, the Cr line will introduce a phase shift of approximately $-\pi/9$ radians (delay versus vacuum). In this case, the positive ZZP, which introduces a $+\pi/2$ phase shift to the 0th order, will partially cancel the contribution from diffracted light, thus rendering the Cr line darker and introducing a contrast enhancement as observed. On the other hand, the $-\pi/2$ phase shift introduced by the negative ZZP will be able to add constructively and render the line brighter, resulting in contrast reversal. Halo artifacts as common to Zernike phase contrast images can also be seen around the ZZP images.

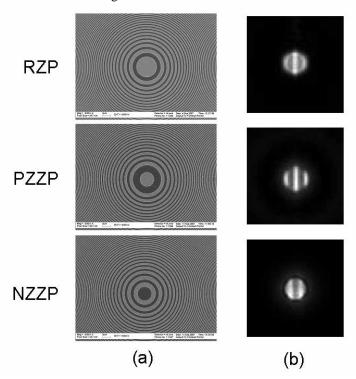


Fig. 4. (a) SEM images of the fabricated regular zone plate (RZP), positive Zernike zone plate (PZZP), and negative Zernike zone plate (NZZP). Each zone plate was fabricated using electron beam lithography with an outermost zone width of 72 nm, 300 zones, and 250 nm thick Ni; (b) Corresponding images obtained with the RZP, PZZP, and NZZP at a wavelength of $\lambda=2.163$ nm using the setup and sample described in Fig. 3. Contrast enhancement is seen in the image taken with the PZZP, and contrast reversal is seen in the image taken with the NZZP.

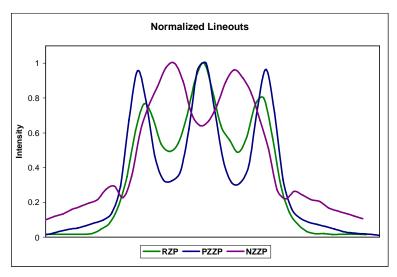


Fig. 5. Normalized line profiles taken horizontally through the center of the regular zone plate (RZP), positive Zernike zone plate (PZZP), and negative Zernike zone plate (NZZP) images in Fig. 4b. The PZZP line profile shows enhanced contrast, and the NZZP line profile shows contrast reversal.

6. Conclusion

Soft x-ray Zernike phase contrast imaging has been performed using positive and negative Zernike zone plates, and contrast enhancement and reversal were observed. Compared to the traditional method of implementing Zernike phase contrast, the phase shift and attenuation imparted to the undiffracted light is no longer coupled to the material properties of a separate phase ring. When attenuation of the undiffracted light is desired to balance the scattering strength of the object, the duty cycle of the shifted zones can be varied. The use of this zone plate provides perfect lateral alignment between the objective zone plate and filter and simplifies alignment since it is a single optical element. Partially coherent x-ray imaging systems can be used in this configuration just as in normal implementation. This method is extendable for use with harder x-rays where many objects are primarily phase objects. It is also useful in the soft x-ray region for contrast enhancement in complex objects, which lowers the image acquisition time and radiation dose on the sample.

Acknowledgements

The authors gratefully acknowledge D. Attwood for stimulating discussions, E. Anderson for alignment help during sample fabrication, and K. Bradley, R. Delano, P. Denham, J. Gamsby, K. Goldberg, E. Gullikson, R. Gunion, H. Huang, M. Jones, C. Kemp, R. Oort, S. Rekawa, and R. Tackaberry for beamline support. This work was supported by the NSF EUV ERC and by the US Department of Energy, Basic Energy Sciences.